International Geology Review, Vol. 44, 2002, p. 797–818.

Prograde and Retrograde P-T Paths of the Late Paleozoic Glaucophane Eclogite from the Renge Metamorphic Belt, Hida Mountains, Southwestern Japan

T. TSUJIMORI[1]

Research Institute of Natural Sciences, Okayama University of Science, Okayama 700-0005, Japan

Abstract

Late Paleozoic glaucophane eclogite and garnet glaucophane schist are intercalated with pelitic schist from the Omi eclogitic unit in the Renge metamorphic belt, Hida Mountains, southwestern Japan. Eclogite and garnet glaucophane schist have MORB-like bulk compositions (major and trace), but garnet glaucophane schist is free from omphacite, reflecting a higher Mg/(Mg+Fe) ratio bulk-rock composition. In the eclogite, three different metamorphic stages (stages I to III) are defined on the basis of microstructures and mineral zoning. In particular, prograde-zoned porphyroblastic garnet preserves the transition from blueschist to eclogite facies. The inclusion trails in the rims of garnet are parallel to a penetrative foliation S_1 in the matrix, and consist of eclogite-facies minerals (omphacite, glaucophane, epidote, rutile, and quartz). Its core contains the preceding epidote blueschist-facies minerals (glaucophane, epidote, titanite, albite, and quartz) instead of eclogite-facies minerals, and has an internal fabric S_0 at a high angle to the surrounding S_1 foliation. In the foliated matrix, the eclogite-facies mineral assemblage garnet + omphacite + glaucophane + epidote + rutile + quartz + phengite is partly replaced by secondary minerals such as chlorite, titanite, albite, and calcite, which coexist with recrystallized glaucophane. These petrographic features show a "hair-pin"-like P-T path that passes from the epidote blueschist facies (stage I) through the eclogite facies (stage II), and then is retraced on a nearly coincident path to epidote blueschist facies (stage III). The systematic decrease from core to rim in K_D value between garnet and omphacite, and a significant increase in jadeite component of omphacite suggest a rise in both temperature and pressure during prograde eclogitization. The host pelitic schist contains the primary mineral assemblage of quartz + paragonite + phengite + garnet + ferroglaucophane + clinozoisite + rutile, and is strongly replaced by secondary albite, chlorite, and titanite. Pseudomorphs after omphacite and possible kyanite are also found in host pelitic schist. Using geothermobarometry for eclogite and a petrogenetic grid for the host pelitic schist, conditions of peak eclogite-facies metamorphism are estimated to be around 550–600°C and at least 1.8 GPa, indicating an apparent paleo-geothermal gradient of ~10°C/km. The eclogite-bearing Renge metamorphic belt in southwestern Japan may be a new candidate for the eastern extension of a suture zone in east-central China. Late Paleozoic blueschist and eclogite metamorphism may be related to subduction of oceanic crust between the Sino-Korean and Yangtze blocks, prior to their collision.

Introduction

DURING THE PAST two decades, much attention has been focused on analyses of the P-T path of low-temperature eclogites, so as to constrain the formation and exhumation of deeply subducted metamorphic rocks at ancient convergence plate margins (e.g. Ernst, 1988). Many retrograde paths have been delineated in P-T space from low-temperature eclogites in Phanerozoic orogens, but there have not been many examples in which the prograde path was decoded. Steady-state thermal models imply that subducting oceanic crust experiences the transition from blueschist to eclogite (Peacock, 1993). This transition is accompanied by the release of a large amount of H_2O, which causes hydration of the overlying mantle wedge (Peacock, 1993; Hacker, 1996). Therefore, the prograde P-T path of low-temperature eclogite provides important limits on the thermal and depth regimes not only for eclogitization of downgoing slabs but also serpentinization of the mantle wedge.

Southwestern Japan, which is a typical circum-Pacific type orogen, contains at least four high-pres-

[1]Corresponding author; email: tatsukix@rins.ous.ac.jp

sure terranes of different ages, which show episodic oceanward growth since Early Paleozoic time (e.g., Isozaki, 1996; Maruyama, 1997). Recently, glaucophane eclogite preserving progressive transition from the epidote blueschist facies to the eclogite facies has been reported from the Omi area of the Late Paleozoic Renge metamorphic belt in the Hida Mountains (Tsujimori et al., 2000a, 2000b). Although the presence of microscopic relics of omphacite has been known in some mafic schists (Nakamizu et al., 1989; Tsujimori and Itaya, 1999), this work has shown for the first time that a regional eclogite-facies metamorphism developed in the Late Paleozoic high-pressure metamorphic belt. This discovery of the Renge eclogite offers a possibility to resolve the regional tectonic correlation between Paleozoic geotectonic units in Japan and Permian–Triassic suture zones in east-central China. Thus, understanding the P-T evolution of the Renge eclogites is integral not only to determining eclogitization processes of subducted materials at ancient convergence plate margins, but also to revealing the crustal development of the eastern margin of the Asian continent. In this paper, the author describes the mineralogic and petrographic characteristics of glaucophane eclogite and associated rocks from the Renge metamorphic belt, Omi area, southwestern Japan, and documents prograde and retrograde P-T paths, with discussion of their significance.

Geologic Setting

Renge metamorphic belt as an older "Sangun" metamorphic belt

The term "Sangun" metamorphic rocks proposed by Kobayashi (1941) had been used for the high-pressure schists that were widely scattered in the Inner Zone of southwestern Japan, western Honshu, northern Kyushu, and the Ryukyu Islands. Before the late 1980s, the "Sangun" metamorphic belt was considered to be a single coherent high-pressure metamorphic belt of pre-Jurassic age, paired with the low-pressure Hida metamorphic belt (e.g., Miyashiro, 1961). However, geochronologic data led to the subdivision of the "Sangun" belt into two discrete geotectonic units: (1) Suo (ca. 230–160 Ma); and (2) Renge (ca. 330–280 Ma) (e.g., Nishimura, 1998; Tsujimori and Itaya, 1999). In the Inner Zone of southwestern Japan, the exposure of Renge schists is limited to several small areas in comparison with the Suo schist (Fig. 1). However, the Renge schist is distributed in small areas along a northwest line from central Kyushu via the Chugoku Mountains to the Hida Mountains. Late Paleozoic high-pressure schists that occur in the Kurosegawa belt of the Outer Zone also are considered as fragments of outliers of the Renge metamorphic belt (e.g., Isozaki, 1996).

Paleozoic rocks in the Hida Mountains

In the Hida Mountains, an eastern portion of southwestern Japan, the Paleozoic rocks comprise two major geotectonic units: (1) the Hida metamorphic belt; and (2) the so-called "Hida marginal zone" (Fig. 2). The Hida metamorphic belt consists of poly-metamorphosed low- to medium-pressure–type orthogneiss, paragneiss, marble, amphibolite, and ferro-aluminous schist (e.g., Miyashiro, 1961; Hiroi, 1981, 1983; Suzuki et al., 1989; Arakawa et al., 2000). This belt is considered as a possible eastern extension of the Triassic suture zone between the Sino-Korean and Yangtze plates (e.g., Isozaki, 1997; Maruyama, 1997). Recent U–Th–total Pb electron microprobe dating of zircon, monazite, and uraninite, and SHRIMP dating of zircon indicate a ~270–210 Ma age of recrystallization during Hida metamorphism (Kunugiza et al., 2001). It has been thought that the Hida belt was thrust southward as a large-scale nappe onto the "Hida marginal belt" (e.g., Komatsu et al., 1993; Sohma and Kunugiza, 1993).

The "Hida marginal zone" is a pre-Jurassic composite geotectonic unit that is tectonically bordered by the Hida metamorphic belt in the north. It consists mainly of fragments of the Oeyama, Renge, Akiyoshi, and Maizuru belts that are more widely developed in the Inner Zone of southwestern Japan (e.g. Komatsu, 1990; Nakamizu et al., 1989) (Fig. 1). Both the serpentinized peridotite of the Oeyama belt and Late Paleozoic high-pressure schist of the Renge belt are the most characteristic components of the "Hida marginal zone." Phengitic mica in the Renge schist gives K-Ar ages of ~330–280 Ma (e.g., Kunugiza et al., 1997). The "Hida marginal zone" is in fault contact with a Jurassic accretionary complex of the Tamba-Mino belt.

Renge schist in the Omi area

The Omi area is located at the northern end of the Hida Mountains and it faces the Japan Sea. In this area, the Renge schist is associated with serpentinite (e.g. Banno, 1958; Matsumoto, 1980; Nakamizu et al., 1989; Tsujimori et al., 2000a) (Fig. 3). The schist is in fault contact with Permo-Carbon-

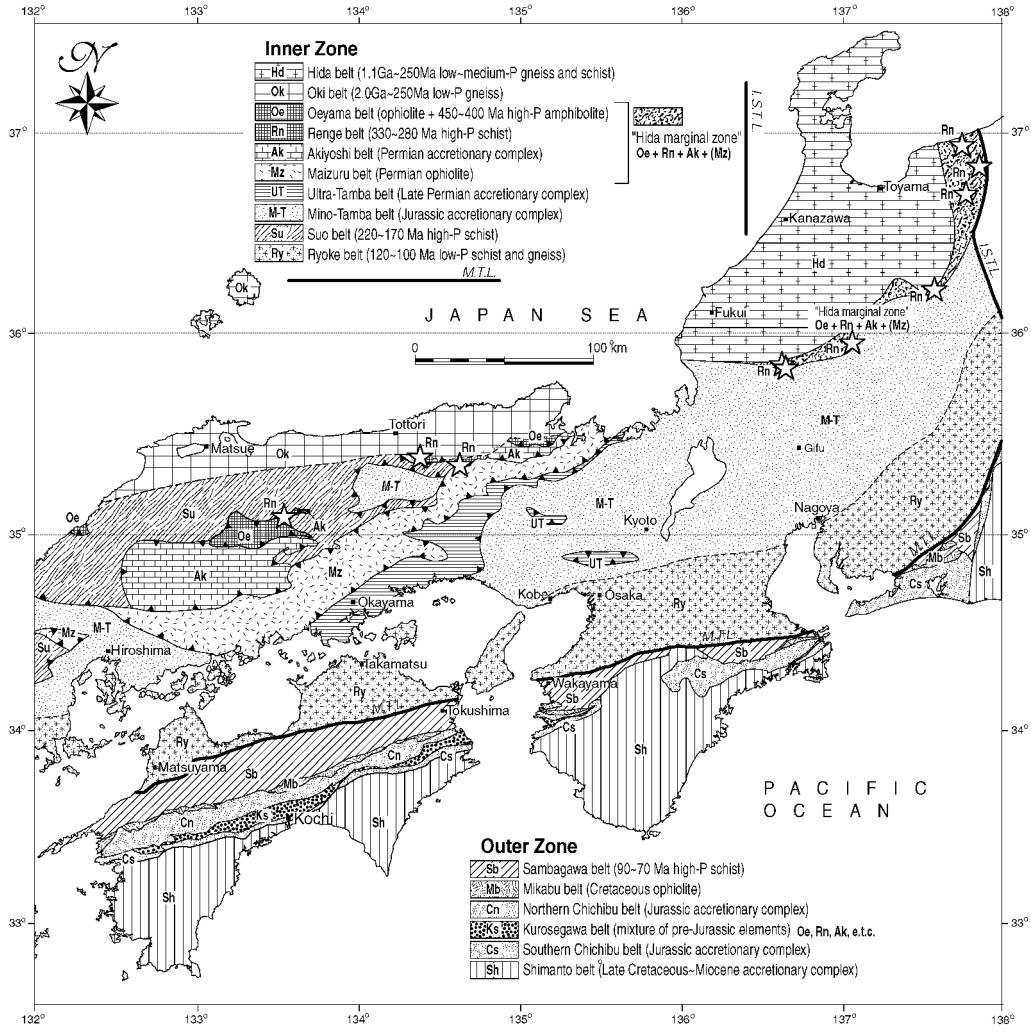

FIG. 1. Geotectonic subdivision of southwestern Japan (modified after Tsujimori and Itaya, 1999). Localities of the Renge blueschists are shown by stars.

iferous accreted sediments (the Omi limestone Group and the Himekawa Group) and Lower Jurassic molasse-type sediments (the Kuruma Group). The schist was divided into the chlorite and biotite zones by the mineral assemblages of pelitic and psammitic schists (Banno, 1958). The biotite-zone schist is sandwiched between two chlorite zones. Several occurrences of glaucophane schist were reported from the chlorite zone (Banno, 1958). Glaucophane eclogite was found from Banno's (1958) southern chlorite zone (Tsujimori et al., 2000a; 2000b). Serpentinite intruded into the schists and along faults between the Kuruma Group and the schists, as well as along the fault in the Permo-Carboniferous formations. The Cretaceous molasse-type sediments of the Tetori Group unconformably overlie all these rocks. Renge schists consist mainly of metasediments (pelitic, psammitic, and siliceous schists) and metabasites with minor amounts of metagabbro. Protolith were trench-fill sediments and fragments of oceanic crust. The phengite K-Ar ages of these schists yield around 330–280 Ma (e.g., Shibata and Nozawa, 1968; Kunugiza et al., 1997).

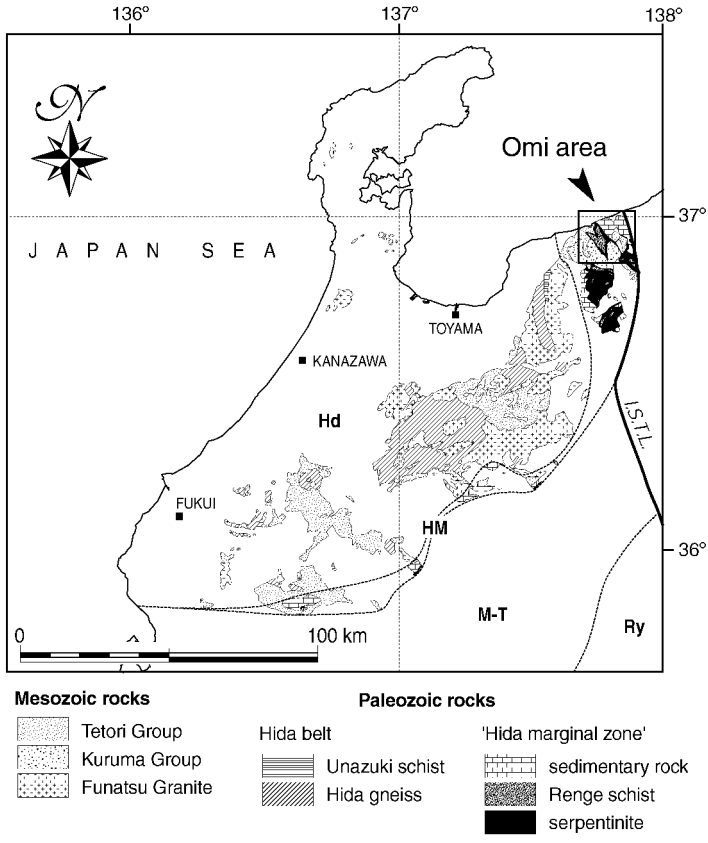

FIG. 2. Distribution map of Paleozoic and Mesozoic rocks in the Hida Mountains, Japan (modified from Suzuki et al, 1989 and Sohma and Kunugiza, 1993).

In the Omi area, the schist is divided into two fault-bounded units, namely an eclogitic unit and a non-eclogitic unit. The eclogitic unit corresponds to Banno's (1958) southern chlorite zone, where a key bed of garnet-rich pelitic schist (20–50 m in thickness) was traced for more than 6 km. In this unit, the glaucophane-bearing metabasites are locally intercalated with micaceous schist. The non-eclogitic unit is compared to Banno's (1958) biotite zone and northern chlorite zone. Preliminary phengite ^{40}Ar-^{39}Ar and K-Ar ages for pelitic and mafic schists from the eclogitic unit give 343 and 348 Ma, respectively (Tsujimori et al., 2001). They are significantly older than previously known K-Ar phengite ages of the non-eclogitic unit mentioned above.

Analytical Methods

Bulk chemical composition

Major (Si, Ti, Al, Fe, Mn, Mg, Ca, Na, K, and P) and trace (Ni, Cu, Zn, Pb, Y, and V) elements were measured by a Rigaku System 3270 X-ray fluorescence spectrometer with Rh tube at the Faculty of Science, Kanazawa University. Operating conditions for both major and trace elements were 50 kV accelerating voltage and 20 mA beam current. Other trace elements (Sc, Cr, Co, Rb, Sr, Zr, Nb, Ba, La, Ce, Sm, Eu, Yb, Lu, Hf, Ta, and Th) were determined by instrumental neutron activation analysis (INAA method). The INAA samples were activated at the Kyoto University Reactor, and their gamma-

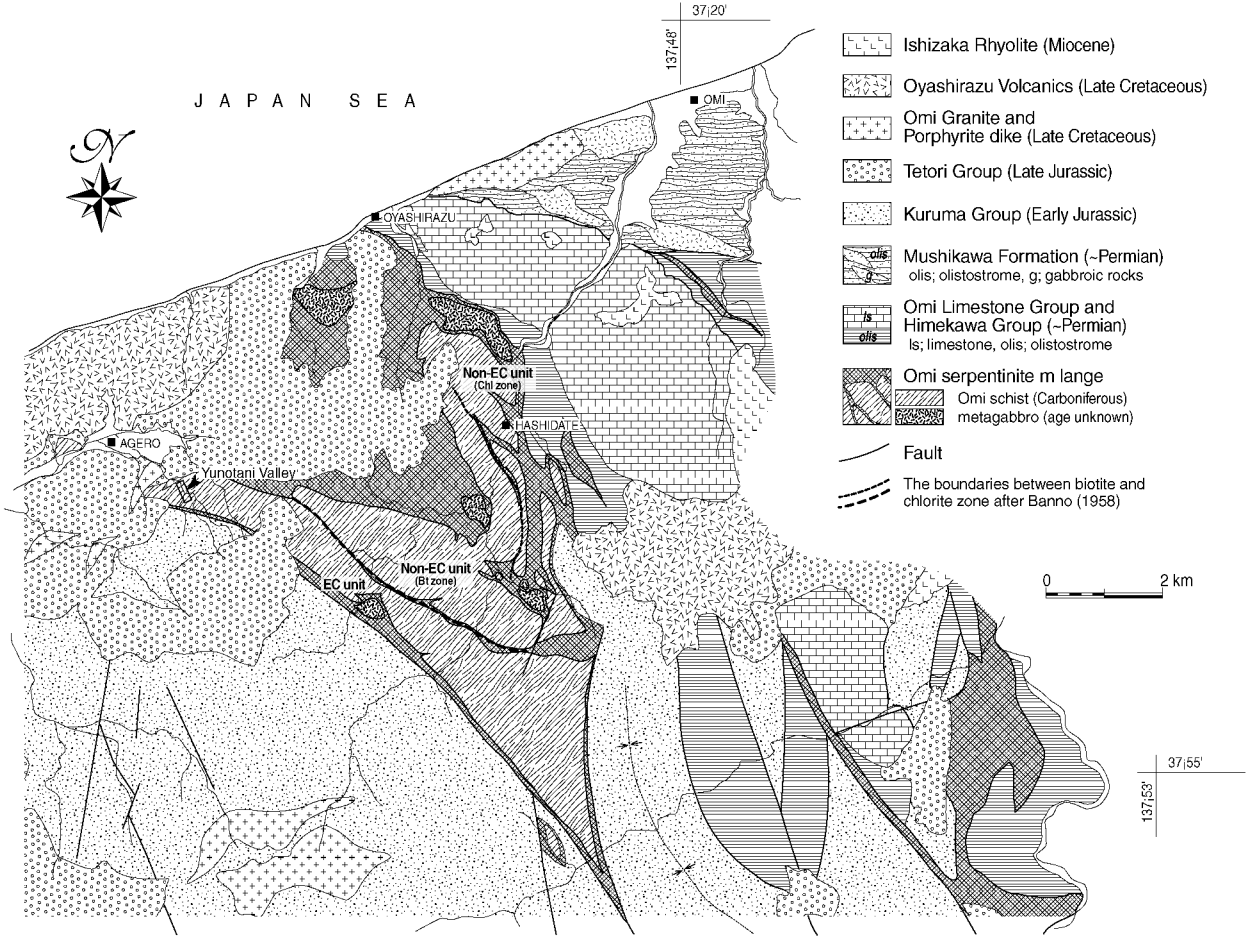

FIG. 3. Geologic map of the Omi area (mapped by Tsujimori, referring to Banno, 1958; Matsumoto, 1980; Kumazaki and Kojima, 1996). Bold broken lines represent the boundary between Banno's (1958) metamorphic zones.

ray spectroscopic analyses were done at the Radioisotope Laboratory of Kanazawa University.

Mineral compositions

Electron microprobe analysis and X-ray element mapping were carried out with a JEOL JXA-8800R at Kanazawa University and JEOL JXA-8900R at Okayama University of Science. The quantitative analyses of rock-forming minerals were performed with 15 kV accelerating voltage, 12 nA beam current and 3 μm beam size. Both electron microprobes have five wave-dispersive spectrometers with dual crystals. Natural and synthetic silicate and oxides were used for calibration. The ZAF method was employed for matrix corrections. The X-ray element maps were collected at 20 kV accelerating voltage and 500 nA beam current, and 120 ms pixel^{-1} count time.

Sample Description and Bulk Chemical Composition

In this study, samples were collected from the Yunotani Valley in the western part of the eclogite unit (Fig. 3). The samples include metabasites and metapelites. The metabasites are subdivided according to their mineral assemblage into three rock types: (1) eclogite (eclogitic glaucophane schist); (2) garnet glaucophane schist; and (3) epidote glaucophane schist. The eclogite contains garnet + omphacite coexisting with glaucophane. The modal abundance of garnet + omphacite locally reaches up to 70%, but is mostly less than 40%. In this paper, the author uses "eclogite" to indicate any metabasite in which garnet and omphacite coexist. The eclogite is typically associated with garnet glaucophane schist. The modal composition of constituent minerals and degree of retrogression are variable from sample to sample. The garnet glaucophane schist is free from omphacite because of the effect of Mg-richer and Ca-poorer bulk compositions, as described below. The epidote glaucophane schist is a well-foliated metabasite, and is significantly finer grained than eclogite and garnet glaucophane schist. In rare cases, this rock type contains relict garnet. This may be a hydrated and recrystallized equivalent of eclogite or garnet glaucophane schist. The detailed petrology of epidote glaucophane schist will be described elsewhere.

Four samples of metabasites and one sample of metapelite were selected for geochemical study. Analyzed bulk-compositional data are given in Table 1. Major-element chemistry shows that the eclogites are basaltic in composition (50.5–51.4 wt% SiO_2), and are characterized by high Al_2O_3 (14.4–15.6 wt%), and moderate CaO (8.4–9.3 wt%), FeO* (11.6–13.6 wt%), Na_2O (2.2–3.0 wt%), and TiO_2 (1.6–2.2 wt%), and low MnO (0.18–0.23 wt%) and P_2O_5 (0.14–0.21 wt.%). Mg# [= $Mg/(Mg+Fe_{total}$ atomic ratio] ranges from 0.41 to 0.49. The garnet glaucophane schist has a basaltic composition (resembling eclogites), but it should be pointed out that is characterized by significantly higher Mg# (0.55) and lower Ca (7.1 wt% CaO) than that of the accompanying eclogite. Similar effects of bulk rock composition on mineral parageneses have been reported from the other low-temperature eclogites (e.g. Schliestedt, 1986; Krogh et al., 1994; Gómez-Pugnaire et al., 1997). The epidote glaucophane schist is also basaltic in composition, with Mg# = 0.41. The relationships of Zr (98–128 ppm) versus Zr/Yi (2–3) and Nb/Y (0.1–0.2) versus Ti/Y (220–282) suggest a MORB-like affinity for our all metabasite samples (Pearce, 1982, 1983). N-MORB–normalized incompatible-element patterns are shown in Figure 4A. Most metabasites show enrichment of Rb, Ba (except for epidote glaucophane schist), and Th. Eclogites show slight enrichment of Sr and depletion of K. The absence of significant Nb and Ta anomalies suggests that the protolith is not correlated with subduction-related calc-alkaline magmatism (Sun and McDonough, 1989). Chondrite-normalized REE patterns are presented in Figure 4B. All metabasites show almost flat or slightly LREE depleted patterns, but relative enrichment in overall REE abundance. These patterns and the absence of a significant Eu anomaly suggest a MORB-like protolith.

Analyzed pelitic schist (sample PS) is the host rock of eclogite [sample EC(a)]. It contains 65 wt% SiO_2, 16 wt.% Al_2O_3, 1.6 wt.% CaO, and 2.8 wt% K_2O. Its Mg# is 0.41 and similar to those of eclogitic rocks. The A value of Thompson's (1957) AFM diagram $[(Al_2O_3 - 3K_2O - Na_2O)/(Al_2O_3 - 3K_2O - Na_2O + FeO^* + MgO)]$ is 0.18. The low-Al feature suggests an origin as trench-fill sediment at an active margin, as in the case of metapelites of the Sambagawa belt in southwestern Japan (Goto et al., 1996).

Petrography and Mineral Chemistry

Eclogites and garnet glaucophane schist

Eclogite and garnet glaucophane schist are medium-grained, layered, and foliated metabasites.

TABLE 1. Bulk Compositions of Eclogites (EC), Garnet Glaucophane Schist (GG), Epidote Glaucophane Schist (EBS), and Metapelite (PS)[1]

Sample	EC(a)	EC(b)	EC(c)	GG	EBS	PS
			wt.%			
SiO_2	50.64	50.49	51.38	50.62	46.94	65.37
TiO_2	1.60	1.64	2.19	1.65	1.85	0.85
Al_2O_3	15.31	15.55	14.39	13.99	15.29	16.06
FeO	11.58	11.91	13.62	12.42	13.63	6.79
MnO	0.18	0.18	0.23	0.15	0.22	0.14
MgO	5.94	6.31	5.35	8.42	5.41	2.70
CaO	9.31	9.10	8.39	7.07	11.87	1.55
Na_2O	2.99	2.78	2.46	3.51	2.18	2.03
K_2O	0.08	0.05	0.06	0.88	0.44	2.80
P_2O_5	0.14	0.19	0.21	0.14	0.18	0.16
Total	97.77	98.20	98.28	98.85	98.01	98.45
Mg#	0.48	0.49	0.41	0.55	0.41	0.41
			Trace elements (ppm)			
Sc	49.1	47.5	46.6	47.5	46.6	49.1
Cr	134	127	68	178	137	99
Co	56	56	59	57	63	33
Ni	64	63	62	72	77	40
Cu	52	57	169	51	27	23
Zn	116	122	111	116	129	94
Rb				17	9	93
Sr	876	842	577	132	253	122
Y	34	35	50	45	51	30
V	310	348	369	371	357	132
Zr	98	100	128	110	118	142
Nb	7	7	8	3	4	9
Pb	7	8	10	2	4	7
Ba	72	27	95	54	4	441
La	6.2	6.7	8.0	3.6	3.6	18.7
Ce	18.4	16.5	20.9	10.2	13.5	40.9
Sm	3.5	3.5	4.5	3.3	3.8	4.3
Eu	1.5	1.4	1.7	1.4	1.4	1.2
Yb	3.4	3.3	4.6	4.4	4.8	2.8
Lu	0.5	0.4	0.6	0.6	0.7	0.5
Hf	2.5	2.8	3.5	3.5	3.9	4.0
Ta			0.7			0.7
Th	0.7	0.7	0.8			6.5

[1] Oxides in wt%, trace elements in ppm; Mg# = $Mg/(Mg+Fe_{total})$ atomic ratio; * = total Fe as FeO.

They occur as centimeter- to meter-size lenses and layers within pelitic schist. The eclogite consists mainly of glaucophane, garnet, omphacite, epidote, and small amounts of quartz, albite, chlorite, rutile, and titanite. In contrast, the garnet glaucophane schist is free of omphacite, but corresponds to a more magnesian and Ca-poorer protolith of eclogite.

A penetrative S_1 foliation defined by preferred orientation of prismatic minerals such as glaucophane and omphacite is characteristically developed. The S_1 foliation overprints the isoclinal fold of compositional layer that is sometimes observed.

Based on the observed microtexture and mineral zoning, three different metamorphic stages (stages I

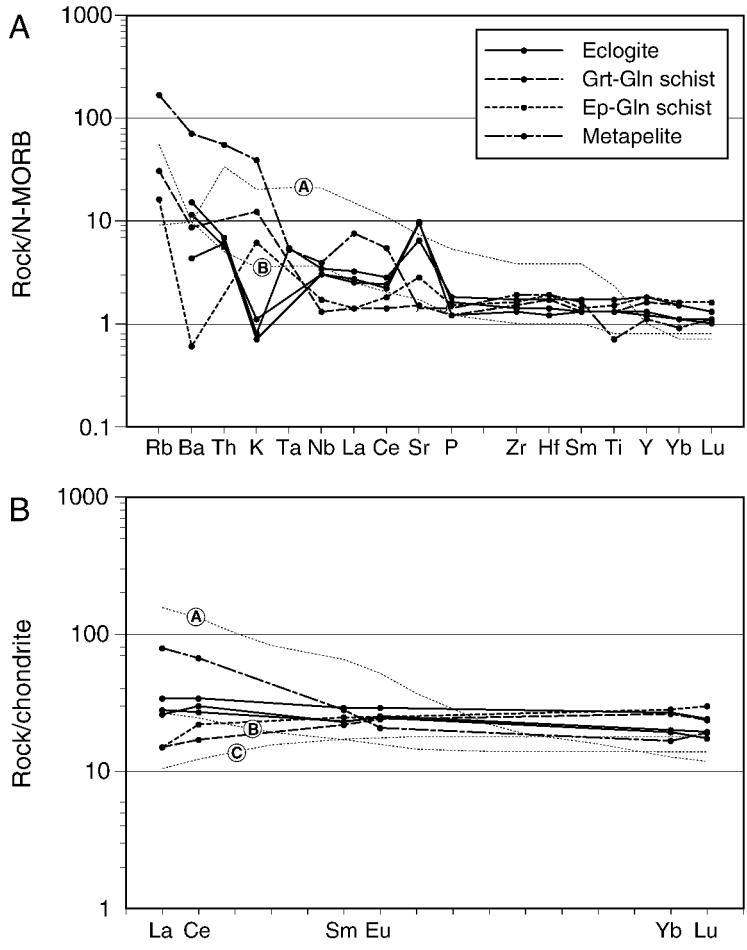

FIG. 4. N-MORB–normalized incompatible-element patterns (A) and chondrite-normalized rare-earth element (REE) patterns (B) for different types of metabasites. The elemental abundance patterns of metapelite associated with eclogites also are shown. Normalizing values are from Sun and McDonough (1989). For comparison, the elemental abundance patterns of Sun and McDonough's (1989) OIB, E-MORB, and N-MORB are also illustrated. Symbols: A = OIB; B = E-MORB; C = N-MORB.

to III) are defined in the eclogite. Summaries of the sequence of mineral parageneses for each stage of evolution are given in Figure 5. Stage I is represented by the assemblage garnet + glaucophane + epidote + titanite + quartz + albite. This stage is only preserved as S_0 inclusion trails within the core of porphyroblastic garnet. Stage II is represented by the assemblage of the matrix: garnet + omphacite + glaucophane + epidote + quartz + rutile ± phengite. Glaucophane coexists with both garnet and omphacite. Stage III minerals replace earlier-stage minerals. In some samples, shear bands crosscutting the S_1 foliation are filled by stage III minerals. These younger shear bands may be consistent with the main foliation of the fine-grained epidote glaucophane schist. This stage is characterized by the assemblage glaucophane (recrystallized) + chlorite + titanite + albite + quartz. In a few samples, glaucophane is rimmed by secondary actinolite. Microstructures and mineral chemistry of minerals (Table 2) are described bellow.

Garnet. Garnet is subhedral to euhedral, 3 to 8 mm in diameter, and is porphyroblastic (Figs. 6A and 6B). Two different inclusion trails are identified in some prograde-zoned garnet (Figs. 6A, 6B, and 7). The inclusion trail in the rims is parallel and

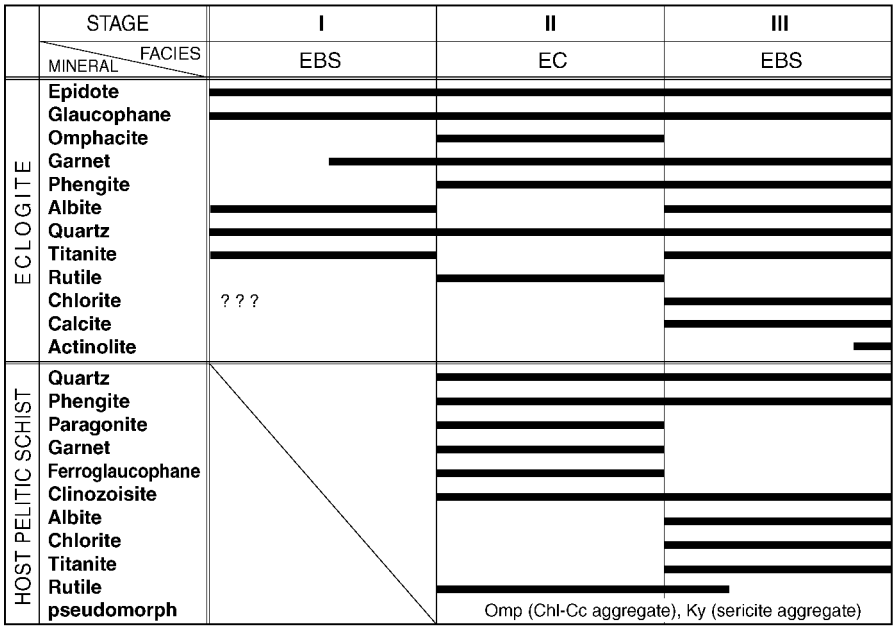

FIG. 5. Mineral parageneses for the different stages of evolution. Abbreviations: EBS = epidote blueschist facies; EC = eclogite facies.

continuous with S_1 foliation in the matrix. It consists of eclogite-facies minerals, including omphacite, rutile, epidote, glaucophane, and quartz (Fig. 6C). Furthermore, omphacite within garnet typically contains glaucophane, quartz, and epidote as inclusions (Fig. 6D). On the other hand, the cores lack inclusions of omphacite and rutile, and have an S_0 internal fabric at a high angle to the surrounding foliation. Epidote, titanite, albite, quartz, and glaucophane occur as S_0 inclusions.

Garnet in eclogite is rich in the almandine (Alm) component with moderate grossular (Grs) and low pyrope (Prp) and spessartine (Sps) (Alm = 48–69%, Grs = 21–36%, Prp = 2–12%, Sps = 0–21%) (Fig. 8). In contrast, garnet in garnet glaucophane schist is plotted on the more magnesian side of the Mg-Fe-Mn ternary diagram, reflecting its Mg-rich bulk chemistry. Garnet shows distinct, prograde, bell-shaped chemical zoning in Mn content (Fig. 9). The Ca content decreases remarkably toward the rim from the transition zone between stage I core and stage II rim. Mg content increases from core to rim, whereas in well-foliated samples, Mg decreases slightly toward the rim from the peak Mg at the inner rim (see zoning profile in Fig. 9).

Omphacite. Omphacite occurs commonly as prismatic or acicular crystals (2–15 mm in length) arranged parallel to the S_1 foliation (Fig. 6C). In the pressure shadow of porphyroblastic garnet, it generally occurs as an aggregate of granular crystals. In rare cases, omphacite is weakly aligned at the hinge of isoclinal folds overprinting the S_1 foliation. Omphacite contains rutile, quartz, epidote, and glaucophane as inclusions. In some samples, omphacite is partly to completely pseudomorphed by fine-grained aggregates of chlorite and calcite.

The Fe^{2+}/Fe^{3+} ratio was estimated on the assumption that total cations = 4, and the end-member components are calculated as jadeite (Jd) = 100 × Al^{VI}/(Ca+Na), aegirine (Ae) = 100 × Fe^{3+}/(Ca+Na), and augite (Aug) = 100 × Ca/(Ca+Na). The nomenclature is based on Morimoto et al. (1988). The omphacite has a composition of Jd = 38–52%, Ae = 5–13% and Aug = 40–53% (Fig. 10A). Coarse-grained omphacite typically shows compositional zoning where the Jd component increases slightly toward the rim. Mg# ranges from 0.62 to 0.86. There is no major difference in the chemical compositions between inclusion and matrix omphacite. However, the Fe-Mg distribution coefficient,

TABLE 2. Representative Electron Microprobe Analyses of Rock-Forming Minerals of Eclogite[1]

	garnet			omphacite		glaucophane			epidote			coexisting pairs in contact						
wt.%	rim	rim	core	rim	core	matrix	S_0 incl.	S_1 incl.	matrix	S_0 incl.	S_1 incl.	[Grt host	Omp] incl.	[Grt rim	Omp] rim	[Grt rim	Omp rim	Phe] rim
SiO_2	37.77	38.44	38.16	56.81	56.83	58.06	57.51	56.67	39.07	38.84	39.63	38.35	55.48	38.41	56.70	38.08	56.44	51.78
TiO_2	0.01	0.01	0.04	0.00	0.00	0.00	0.00	0.00	0.04	0.01	0.00	0.00	0.01	0.00	0.06	0.01	0.00	0.03
Al_2O_3	21.65	21.29	21.40	12.39	10.33	11.47	11.48	11.91	27.39	26.99	27.99	21.22	10.54	21.44	11.13	21.13	10.67	26.60
Cr_2O_3	0.02	0.00	0.01	0.00	0.01	0.01	0.00	0.02	0.00	0.06	0.00	0.00	0.08	0.00	0.00	0.01	0.00	0.00
Fe_2O_3	–	–	–	–	–	–	–	–	8.53	9.07	6.88	–	–	–	–	–	–	–
FeO	28.21	27.73	24.82	6.88	8.06	10.64	10.52	11.06	–	–	–	27.24	7.57	28.90	7.73	27.57	7.54	2.01
MnO	0.44	0.61	3.39	0.00	0.00	0.00	0.05	0.03	0.00	0.24	0.28	0.40	0.00	0.63	0.00	0.55	0.00	0.00
MgO	2.31	2.77	1.30	5.37	6.35	9.80	9.87	9.79	0.05	0.00	0.01	2.42	6.48	2.47	5.88	2.26	6.63	3.34
CaO	9.66	9.56	11.32	10.42	12.56	0.71	1.13	1.05	23.16	23.13	23.95	10.30	11.97	8.93	11.24	9.84	11.25	0.04
Na_2O	0.04	0.09	0.00	8.64	7.67	7.21	6.80	7.07	0.00	0.05	0.00	0.01	7.84	0.04	8.21	0.05	7.89	0.57
K_2O	0.00	0.00	0.01	0.00	0.00	0.00	0.00	0.04	0.00	0.00	0.01	0.01	0.02	0.01	0.01	0.00	0.01	9.81
Total	100.12	100.48	100.44	100.50	101.80	97.90	97.35	97.63	98.24	98.40	98.76	99.95	99.99	100.83	100.96	99.49	100.43	94.17
									Atomic ratios									
O=	12	12	12	4	4	23	23	23	25	25	25	12	4	12	4	12	6	22
Si	2.988	3.021	3.014	2.010	2.002	7.937	7.904	7.789	6.061	6.040	6.099	3.028	1.981	3.018	2.006	3.026	2.006	6.941
Ti	0.000	0.000	0.003	0.000	0.000	0.000	0.000	0.000	0.005	0.001	0.001	0.000	0.000	0.000	0.002	0.000	0.000	0.003
Al	2.019	1.973	1.992	0.516	0.429	1.849	1.859	1.929	5.008	4.946	5.078	1.975	0.444	1.986	0.464	1.979	0.447	4.202
Cr	0.001	0.000	0.001	0.000	0.000	0.001	0.000	0.002	0.000	0.008	0.000	0.000	0.002	0.000	0.000	0.001	0.000	0.000
Fe^{3+}	–	–	–	0.056	0.090	0.158	0.188	0.290	0.995	1.062	0.797	–	0.135	–	0.084	–	0.085	–
Fe^{2+}	1.867	1.822	1.639	0.147	0.147	1.058	1.021	0.981	–	–	–	1.799	0.091	1.899	0.145	1.832	0.139	0.225
Mn	0.030	0.040	0.227	0.000	0.000	0.000	0.006	0.003	0.000	0.031	0.037	0.027	0.000	0.042	0.000	0.037	0.000	0.000
Mg	0.273	0.324	0.153	0.283	0.333	1.997	2.021	2.005	0.012	0.000	0.001	0.284	0.345	0.289	0.310	0.268	0.351	0.667
Ca	0.819	0.805	0.958	0.395	0.474	0.103	0.166	0.155	3.850	3.854	3.950	0.871	0.458	0.752	0.426	0.837	0.428	0.006
Na	0.006	0.013	0.000	0.592	0.524	1.911	1.812	1.884	0.000	0.016	0.000	0.002	0.543	0.005	0.563	0.008	0.543	0.148
K	0.000	0.000	0.001	0.000	0.000	0.000	0.000	0.007	0.000	0.000	0.003	0.001	0.001	0.001	0.000	0.000	0.000	1.676
Total	8.004	7.999	7.987	4.000	4.000	15.014	14.978	15.046	15.932	15.959	15.964	7.986	4.000	7.992	4.000	7.988	4.000	13.868

[1] Coexisting mineral rims in contact with each other are also listed. S_0 and S_1 represent inclusions within garnet cores and rims, respectively; * = total Fe as FE_2O_3; ** = total Fe as FeO.

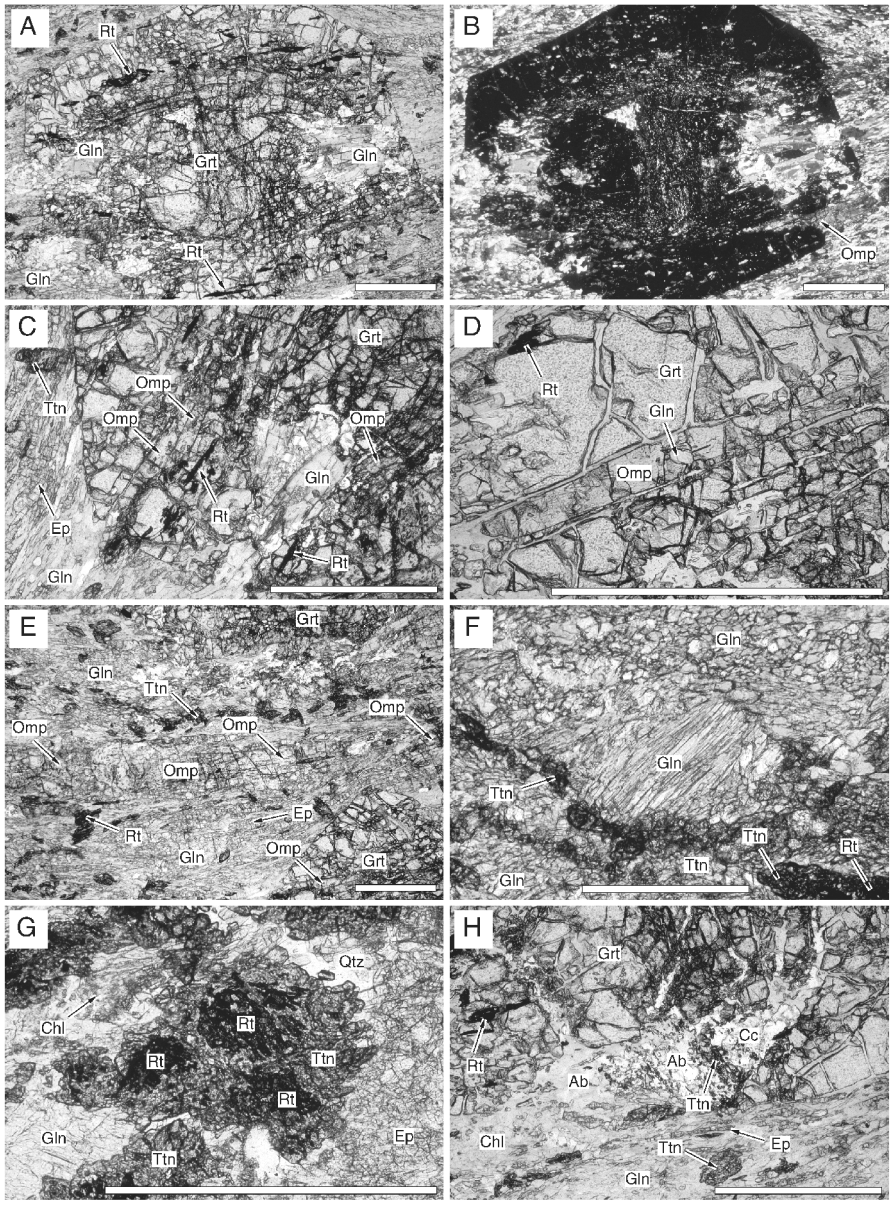

FIG. 6. Photomicrographs showing textural relationship of minerals in eclogite. A. Porphyroblastic garnet with two different inclusion trails. The inclusion trail in the rim is continuous with S_1 foliation in the matrix. The core has an internal fabric S_0 at a high angle to the surrounding foliation; plane-polarized light. B. The same view as Figure 6A; cross-polarized light. C. Eclogite-facies inclusions within a porphyroblastic garnet. The inclusions are strongly oriented parallel to the foliation S_1; plane-polarized light. D. Prismatic omphacite included within porphyroblastic garnet. The omphacite contains rounded glaucophane grains as inclusions; plane-polarized light. E. Coarse-grained omphacite oriented parallel to the foliation S_1; plane-polarized light. F. Lenticular aggregates of coarser-grained glaucophane enclosed by finer-grained recrystallized glaucophanes; plane-polarized light. G. Rutile corroded by aggregates of fine-grained titanite; plane-polarized light. H. Secondary albite coexisting with chlorite and calcite adjacent to a garnet porphyroblast; plane-polarized light. Abbreviations: Ab = albite; Cc = calcite; Chl = chlorite; Ep = epidote; Gln = glaucophane; Grt = garnet; Omp = omphacite; Rt = rutile; Qtz = quartz; Ttn = titanite. The scale bar in each photomicrograph = 1.0 mm.

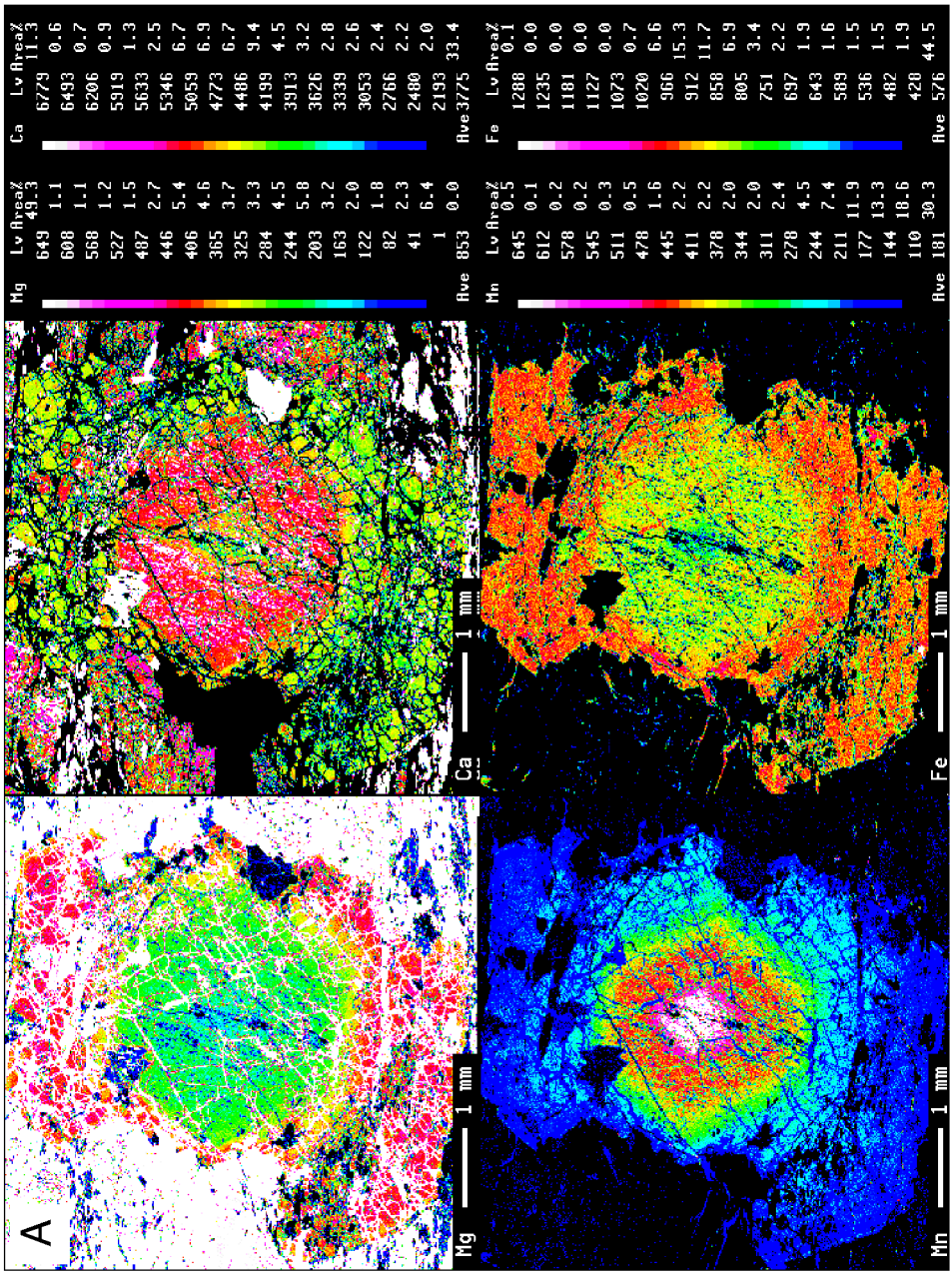

FIG. 7. A. Mg, Ca, Mn, and Fe X-ray element maps of a porphyroblastic garnet.

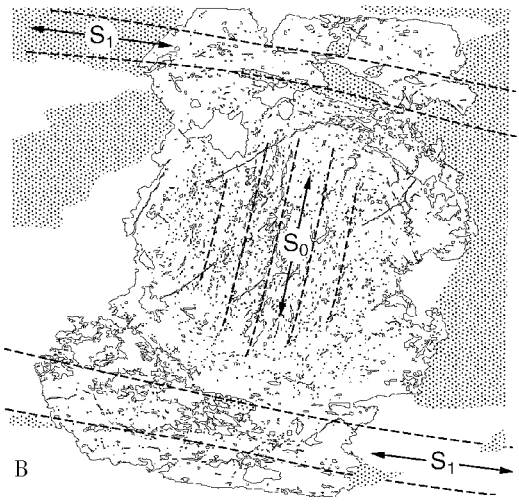

FIG. 7. B. Sketch of a porphyroblastic garnet (same view as Fig. 7A). Two kinds of fabric are traced by dashed lines. See the text for description. The shaded area represents omphacite.

K_D (= $(Fe/Mg)_{Grt}/(Fe/Mg)_{Omp}$), between omphacite inclusions and adjacent garnet shows a tendency to be significantly larger than that of matrix pairs (Fig. 10B).

Na amphibole. Glaucophane occurs as nematoblasts parallel to S_1 (mostly < 1 mm in length), and as tiny inclusions (< 0.1 mm) within porphyroblastic garnet and omphacite. In the weakly deformed part, coarse-grained glaucophane (up to 6 mm) occurs and coexists with omphacite. Glaucophane does not replace omphacite. In rare cases, lenticular aggregates of coarser-grained glaucophane are wrapped around by layers of finer-grained, recrystallized glaucophane (Fig. 6F), indicating that initially coarser-grained glaucophane underwent grain-size reduction by recrystallization during deformation. Such recrystallized glaucophane generally coexists with secondary minerals, i.e., stage III phases, such as chlorite, titanite, and albite.

The structural formulae of amphiboles were calculated based on 23 oxygens, and the Fe^{2+}/Fe^{3+} ratio was estimated on the assumption of a total of 13 cations (O = 23) excluding Ca, Na, and K. The nomenclature of Na amphibole is based on Leake (1978). Na amphiboles in eclogite are mostly glaucophane with X_{Fe2+} (= $Fe^{2+}/(Fe^{2+}+Mg)$) = 0.28–0.46 and X_{Fe3+} (= $Fe^{3+}/(Fe^{3+}+Al)$) < 0.20 (Fig. 11). Glaucophane is low in Ca (average 1.0 wt% CaO). Ferroglaucophane with X_{Fe2+} = 0.41–0.45 and $Fe^{3+}/(Fe^{3+}+Al)$ = 0.19–0.22 occurs at some interfaces between glaucophane and garnet from one thin section. Glaucophane of the S_0 fabric within garnet cores has a composition with X_{Fe2+} = 0.34–0.39 and X_{Fe3+} < 0.16. There is no difference in compositions between coarse-grained glaucophane and finer-grained recrystallized glaucophane of the later stages. Glaucophane in garnet glaucophane schist is plotted on the lower X_{Fe2+} side on Miyashiro's (1957) diagram, reflecting its Mg-rich bulk composition.

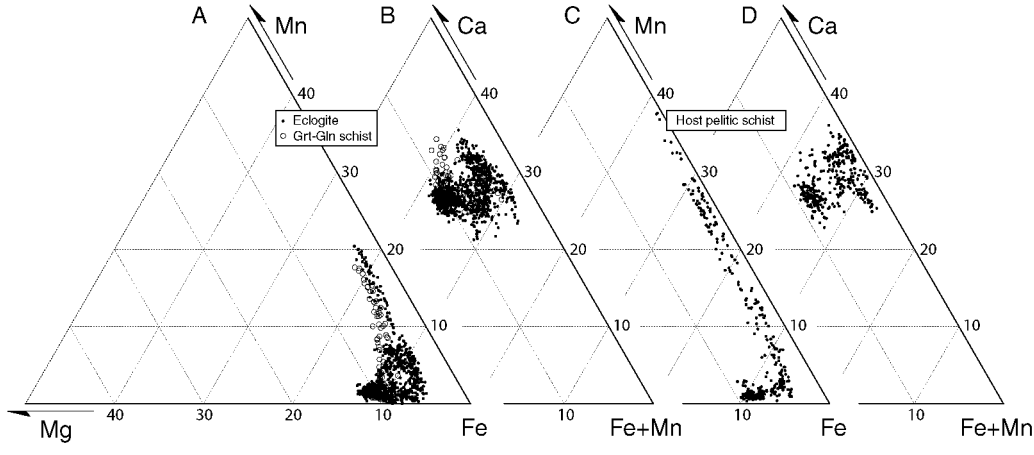

FIG. 8. Chemical compositions of garnets in Mn-Fe-Mg and Ca-(Fe+Mn)-Mg ternary diagrams. A and B. Eclogite and garnet glaucophanite. C and D. Host pelitic schist.

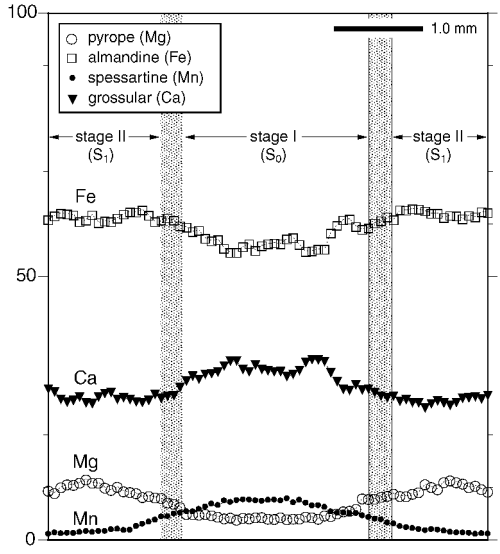

FIG. 9. Representative zoning profiles of garnet with S_0 core from well-foliated eclogite sample.

Epidote. Epidote occurs commonly as discrete fine-grained prisms (< 0.5 mm in length) and as mosaic aggregates. The X_{Fe3+} of epidote in the matrix ranges from 0.11 to 0.27. The X_{Fe3+} of epidote in the S_0 inclusion trail within garnet cores is 0.11–0.25, and that of the S_1 inclusion fabric at the garnet rim is 0.12–0.20.

Other minerals. Phengite occurs as lepidoblasts or aggregates in contact with garnet and omphacite in some samples. Phengite has 6.8–7.1 Si p.f.u. (O = 22), and the Na/(Na+K) ratio varies from 0.08 to 0.17. Mg# ranges from 0.62 to 0.73, and shows a positive correlation with Si content.

Rutile in the foliated matrix is partially replaced by titanite, whereas rutile inclusions within garnet and omphacite survive replacement by titanite (Fig. 6G). In rare cases, large rutile crystals up to 5 mm long are present. Rutile contains 0.2–0.6 wt% Fe_2O_3.

Stage III titanite coexists with secondary albite, chlorite, calcite, and recrystallized glaucophane. It contains significant Al_2O_3 (1.0–2.8 wt%) in solid solution. No compositional difference between stage I and stage III titanite is observed.

Albite fills cracks in porphyroblastic garnet, and replaces the margins of porphyroblastic garnet. It commonly accompanies chlorite, titanite, and cal-

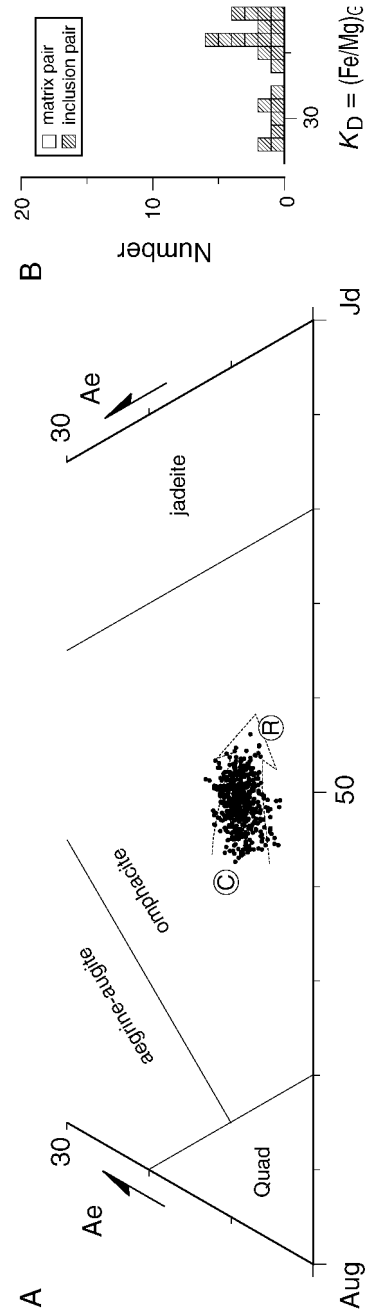

FIG. 10. A. Chemical compositions of omphacite in Morimoto's (1988) quad-jadeite-aegirine ternary system. B. Histogram of Fe-Mg distribution coefficient, K_D (= $(Fe/Mg)_{Grt}$/$(Fe/Mg)_{Omp}$), between garnet and omphacite.

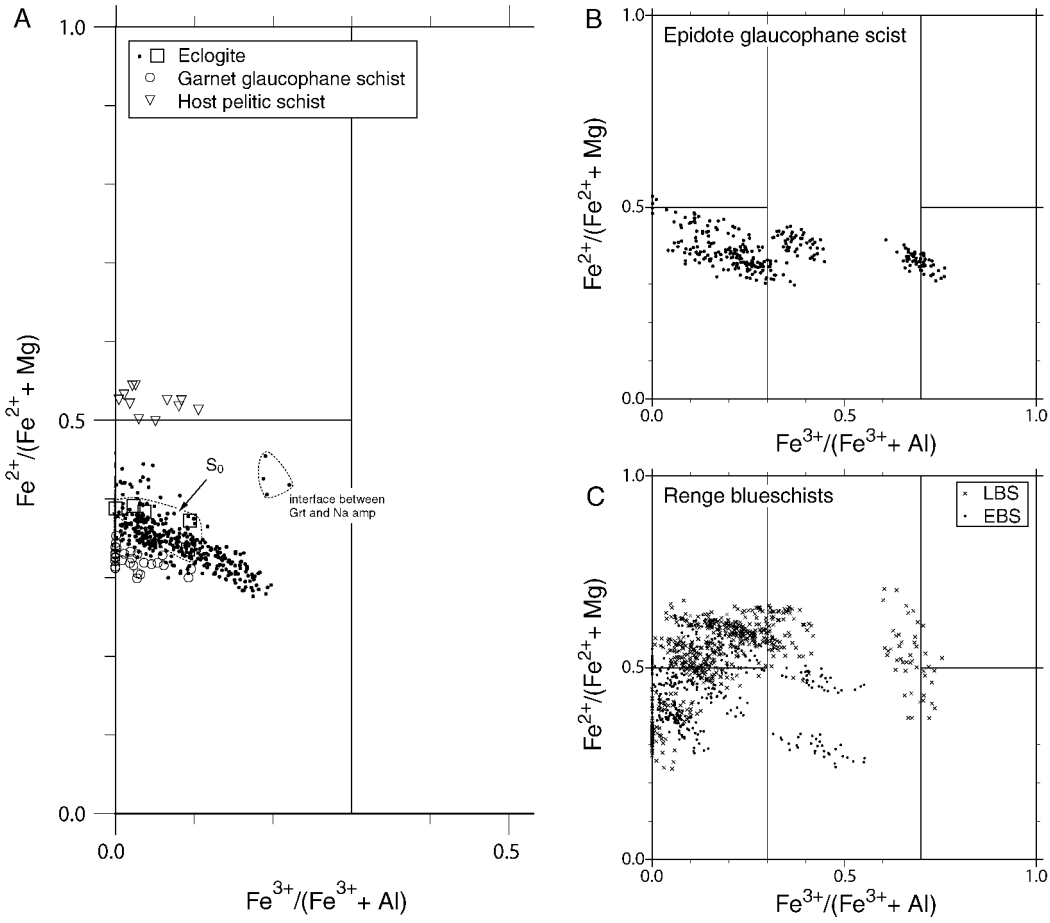

FIG. 11. Chemical compositions of Na amphiboles in Miyashiro's (1957) $Fe^{3+}/(Fe^{3+}+Al)$ versus $Fe^{2+}/(Fe^{2+}+Mg)$ diagram. A. Na amphibole in eclogite, garnet glaucophanite, and host pelitic schist. B. Na amphibole in epidote glaucophane schist in the Omi area. C. Na amphiboles from Renge blueschist at other localities (data compiled from Tsujimori, 2001).

cite (Fig. 6H). It has a pure albite composition with $X_{An} < 0.01$.

Chlorite occurs as a stage III mineral, with Mg# = 0.51–0.60. Secondary chlorite in garnet glaucophane schist is enriched in Mg (Mg# = 0.56–0.66).

Secondary actinolite overgrowing on glaucophane has a composition with Mg# = 0.62–0.72. $Na_{(B)} = 0.11–0.29$.

Host pelitic schist

The host pelitic schist is coarse grained and micaceous. Porphyroblastic garnet is scattered in the matrix, and consists mainly of phengite, paragonite, quartz, albite, garnet, and minor chlorite, rutile, titanite, and apatite. Ferroglaucophane, clinozoisite, and graphite occur in some samples. The assemblage paragonite + garnet + phengite + clinozoisite + ferroglaucophane + quartz + rutile is the primary assemblage that is equivalent to stage II eclogite-facies metamorphism.

Garnet is subhedral to euhedral, and contains tiny quartz and rutile inclusions. Most garnets are extensively replaced by secondary chlorite and albite. Garnet is rich in almandine component with moderate grossular and spessartine, and low pyrope (Alm = 32–38%, Grs = 23–36%, Prp = 1–10%, Sps = 1–38%) (Fig. 8). It shows distinct, prograde, bell-shaped chemical zoning in Mn content. Paragonite is lepidoblastic (0.1–2 mm in size) in the matrix and

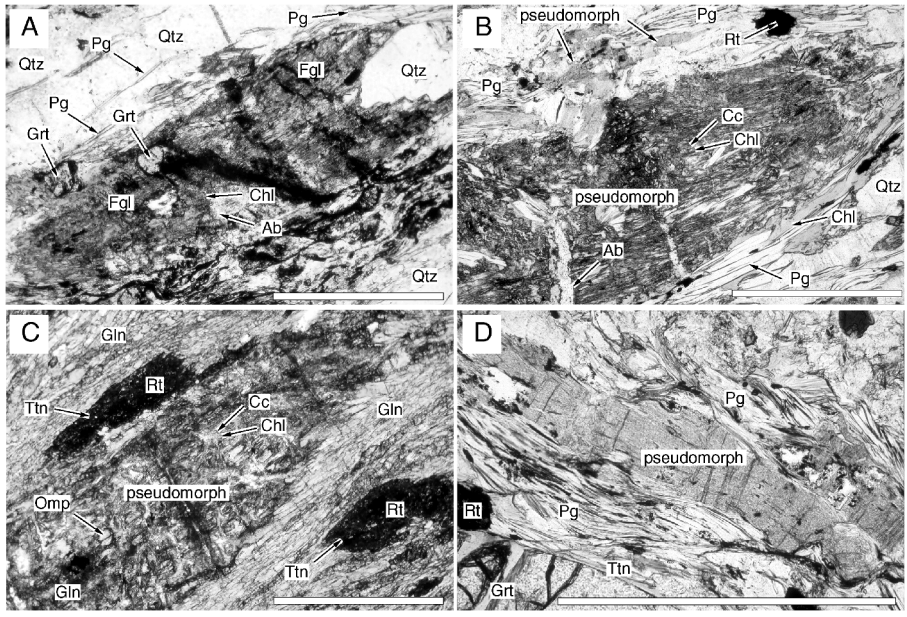

FIG. 12. Photomicrographs showing textural relationship of minerals in host pelitic schist (except for Fig. 12C). A. Ferroglaucophane coexisting with garnet and paragonite. B. Pseudomorph after omphacite (pseudomorph1), consisting of fine-grained aggregates of chlorite and calcite. See next picture for comparison. C. Pseudomorph after omphacite in eclogite. Omphacite still remains, although it is severely replaced by chlorite and calcite. D. Very fine grained aggregates of muscovite (pseudomorph 2), possible pseudomorph after kyanite; plane-polarized light. Abbreviations: Ab = albite; Cc = calcite; Chl = chlorite; Fgl = ferroglaucophane; Grt = garnet; Omp = omphacite; Pg = paragonite; Phe = phengite; Rt = rutile; Qtz = quartz; Ttn = titanite. The scale bar in each photomicrograph = 1.0 mm.

most is intergrown with lepidoblastic phengite. Paragonite has a composition with Na/(Na+K) = 0.85–0.97; phengite has 6.7–7.0 Si p.f.u. (O = 22); and the Na/(Na+K) ratio varies from 0.01 to 0.15. Some clinozoisite (X_{Fe3+} = 0.16–0.18) coexists with paragonite in the micaceous matrix. Ferroglaucophane coexisting with garnet and paragonite (Fig. 12A) has a composition with (X_{Fe2+} = 0.50–0.54 and X_{Fe3+} < 0.11) (Fig. 11). It is often replaced partly by secondary chlorite and albite. Two kinds of pseudomorph after some prismatic minerals are observed in some samples. One of them consists of fine-grained aggregates of chlorite and calcite (Fig. 12B). The author considers that this is pseudomorphic after omphacite, because the chlorite + calcite aggregate resembles already confirmed pseudomorphs after omphacite in the eclogite. The other consists of very fine grained aggregates of muscovite (Fig. 12D). The author considers this to be sericitic alteration of kyanite. In the host pelitic schist, both rutile and titanite occur as discrete crystals. Even if rutile is sometimes replaced by titanite, there are no contrary textual relations.

Metamorphic Conditions

Stage I: Early prograde, blueschist-facies metamorphism

Stage I represents the early prograde history, characterized by the assemblage garnet + glaucophane + epidote + titanite + albite + quartz that is preserved at the core of garnet. Although geothermometers based on Fe-Mg exchange reactions are not applicable for this stage, its approximate P-T condition can be deduced by petrogenetic grids for mineral equilibrium. In the petrogenetic grid for metabasite in the system Na_2O-CaO-MgO-Al_2O_3-SiO_2-H_2O, the glaucophane + epidote paragenesis is stable in the epidote blueschist facies (e.g., Evans, 1990). In addition, it is inferred that stage I inclusions were in equilibrium with adjacent garnet. The appearance of almandine-rich garnet in epidote

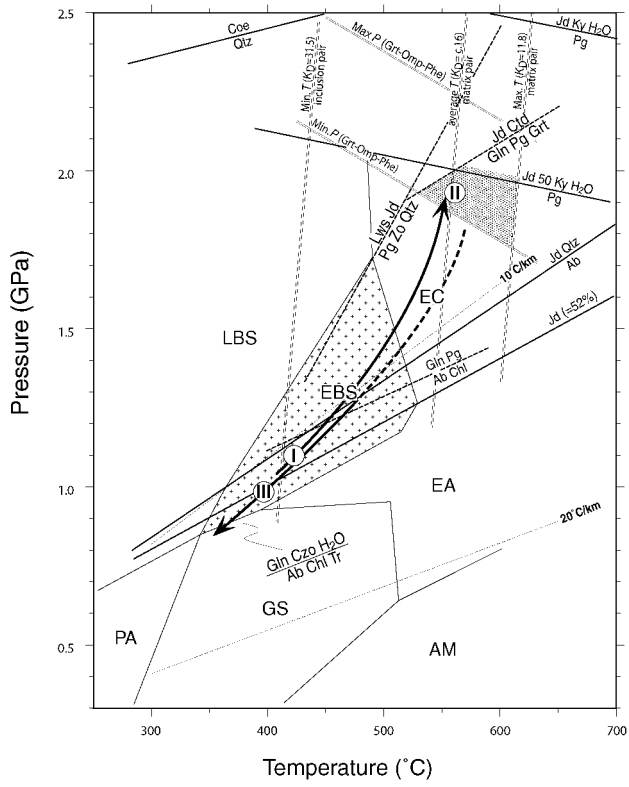

FIG. 13. Pressure-temperature diagram showing the P-T path (solid arrow) of the Renge eclogite. The hatched area represents the estimated eclogite-facies condition. The petrogenetic grid for Na amphibole composition (a_{Gln} = 0.073) proposed by Evans (1990) is used to constrain the stability field of the epidote blueschist facies (hatched with small crosses). Double lines show isopleths obtained from garnet-clinopyroxene thermometry (Krogh, 1988) and garnet-omphacite-phengite thermobarometry (Carswell et al., 1997). Dashed lines represent reaction curves in the system Na_2O-CaO-FeO-MgO-Al_2O_3-SiO_2-H_2O showing P-T limits of assemblage paragonite + garnet + clinozoisite + ferroglaucophane, and ferroglaucophane + paragonite (after Guiraud et al., 1990; Guillot et al., 1997). Geothermal gradients of 10°C/km and 20°C/km are shown as dotted lines for reference. Facies abbreviations: LBS = lawsonite blueschist facies, EBS = epidote blueschist facies; PA: pumpellyite-actinolite facies; GS = greenschist facies; EA = epidote amphibolite facies; AM = amphibolite facies. Mineral abbreviations: Ab = albite; Chl = chlorite; Coe = coesite; Ctd = chloritoid; Czo = clinozoisite; Gln = glaucophane; Grt = garnet; Jd = jadeite; Ky = kyanite; Lws = lawsonite; Pg = paragonite; Qtz = quartz; Tr = tremolite; Zo = zoisite.

glaucophane schist with common basaltic composition has been estimated as 400–460°C (e.g., Yokoyama et al., 1986; Patrick and Evans, 1989). The minimum temperature for stage I is therefore likely to be close to the garnet-in isograd. The presence of titanite instead of rutile also is consistent with this broad estimate. The P-T conditions of stage I should be restricted to the albite-stable field in the high-temperature portion of the epidote blueschist facies (Fig. 13).

Stage II: Peak eclogite-facies metamorphism

Stage II represents the late prograde stage and metamorphic peak. This stage is characterized by the assemblage garnet + omphacite + glaucophane + epidote + rutile + quartz. Using the experimental data of Holland (1980) for the equilibrium albite = jadeite + quartz, a minimum pressure is calculated from the jadeite component, assuming ideal jadeite-diopside solid solution. The omphacite (up to 52%

jadeite) + quartz equilibrium in eclogite gives minimum pressure of ~1.2–1.4 GPa at a nominal temperature of 500–600°C. Temperature is estimated from the Fe-Mg partitioning between coexisting garnet and omphacite. As mentioned above, the K_D values of inclusion pairs (31.7–14.9) are significantly greater than that of matrix pairs (20.3–11.8). In addition, the jadeite component increases rimward in the matrix omphacite. These changes indicate a rise in both temperature and pressure during stage II eclogite-facies metamorphism. The maximum K_D value (31.6) of inclusion pairs constrains the minimum temperature of incipient eclogitization of stage II. Application of the garnet-omphacite thermometry of Krogh (1988) yields a minimum temperature of 413–417°C at a nominal pressure of 12–1.4 GPa. The temperature of peak conditions is given by the K_D value of the matrix pair. The K_D value of the matrix pairs is concentrated around an average value of 16. The minimum K_D value (11.8) of a matrix pairs gives a maximum temperature of 606–611°C at a nominal pressure of 1.4–1.6 GPa. The temperature calibrated using the average K_D value is ~550°C at a nominal pressure of 1.3–1.5 GPa (Fig. 13). In some samples, phengite coexists with both garnet and omphacite. This paragenesis allows the application of the garnet-omphacite-phengite barometry of Carswell et al. (1997). Their barometry yields a pressure of ~1.8–2.0 GPa at ~550–600°C (Fig. 13).

Stage III: Blueschist-facies overprinting

Stage III represents retrogression after peak eclogite facies. In the eclogite, the assemblage glaucophane + epidote + chlorite + titanite + albite + quartz ± calcite is limited to the P-T range of the albite-stable, garnet-free, lower-temperature portion of the epidote blueschist facies (e.g., Evans, 1990). As mentioned above, some actinolite overgrowing glaucophane is present in a few samples. This implies that minimum pressure is limited by the transition-boundary reaction between epidote blueschist facies and greenschist facies.

Constraint from host pelitic schist

The paragonite-bearing mineral assemblage in the host pelitic schist is important in constraining a much more restricted P-T condition for stage II. The primary assemblage of stage II in the host pelitic schist is represented by the assemblage quartz + paragonite + phengite + garnet ± ferroglaucophane ± clinozoisite + rutile. According to the petrogenetic grid in the system Na_2O-CaO-FeO-MgO-Al_2O_3-SiO_2-H_2O (e.g., Guiraud et al., 1990; Guillot et al., 1997), the equilibrium lawsonite + jadeite = paragonite + zoisite + quartz + H_2O, and jadeite + chloritoid = garnet + paragonite + glaucophane defines pressure-temperature limits for the assemblage paragonite + garnet + clinozoisite + ferroglaucophane (Fig. 13). As mentioned above, the host pelitic schist contains two kinds of pseudomorph after omphacite and kyanite. The appearance of these pseudomorphs implies that the upper pressure limit reached the location of the equilibrium paragonite = jadeite (50%) + kyanite + H_2O (Holland, 1979).

Discussion

Pressure-temperature path

To summarize the metamorphic evolution of the Renge eclogites and associated rocks in the Omi area, we can delineate a remarkable prograde-retrograde P-T path (Fig. 13). It passes from the epidote blueschist facies (stage I) through the eclogite facies (stage II), and then retraces a nearly coincident trajectory back to the epidote blueschist facies (stage III).

The P-T conditions of stage I are restricted to the albite-stable field in the high-temperature portion of the epidote blueschist facies. The early prograde P-T path lies just below the stability field of jadeite + quartz, and passes through the moderate-temperature portion of the epidote blueschist facies. The S_1 foliation preserved in the garnet cores may be related to deformation during subduction. The P-T conditions for stage II in eclogite are deduced from a combination of geothermobarometry for the eclogite and mineral equilibrium for the host pelitic schist. The systematic changes in K_D between garnet and omphacite, and the significant increase in the jadeite component of omphacite suggest that a temperature increase accompanied the pressure increase. With a rise in both temperature and pressure, the prograde path sailed across the reaction line albite = jadeite + quartz into the jadeite + quartz stability field. The eclogite-facies metamorphism occurred at ~550–600°C and at least 1.8 GPa during subduction. The eclogite-facies deformation formed penetrative S_1 foliation and overprinted the earlier S_0 fabric.

The retrograde P-T path after the eclogite metamorphism is deduced from both the eclogite and host pelitic schist. The late-stage mineral assemblage and breakdown textures define the retrograde

P-T path. In the host pelitic schist, ferroglaucophane is partly replaced by both albite and chlorite. This texture implies a decompression P-T path passing through the equilibrium glaucophane + paragonite = chlorite + albite. In addition, the presence of actinolite overgrowing on glaucophane in eclogite indicates that the decompression P-T path reached transitional conditions between the epidote blueschist facies and the greenschist facies. The inferred retrograde P-T path shows significant refrigeration during decompression, and almost retraces the prograde one. This is similar to that of Ernst's (1988) "Franciscan-type" retrograde path.

Eclogites and associated rocks in the Omi eclogite unit provide evidence for the P-T path leading to the development of eclogite in the Late Paleozoic Renge metamorphism. The bulk compositions of eclogites are consistent with the original rocks existing as MORB. This implies that the Renge eclogite was oceanic crust that underwent prograde eclogitization during subduction. The apparent paleo-geotherm is estimated to be ~10°C/km. The inferred prograde P-T path is similar to that predicted by steady-state thermal models of subduction zones (Peacock, 1993). This can be explained simply by fast subduction of a cold oceanic plate.

Significance of Late Paleozoic eclogite in southwestern Japan

Recent studies on Phanerozoic orogenic belts in central China have shown that the Sino-Korean and Yangtze blocks collided along the Qinling-Dabie suture, generating a high- to ultrahigh-pressure complex (e.g., Ernst et al., 1991; Maruyama et al., 1994; Ernst and Liou, 1995; Wang et al., 1995). The eastward extension of the Qinling-Dabie orogenic belt is manifested by the occurrence of UHP metamorphic rocks in the Sulu region (e.g., Hirajima et al., 1990). Hence, this collisional orogen extends 2000 km from west to east. Farther east, it has been conjectured that the Qinling-Dabie-Sulu belt passes through the Permian–Triassic fold belts in the Korean peninsula and southwestern Japan (e.g., Ernst and Liou, 1995; Ree et al., 1996; Isozaki, 1997; Lee et al., 2000). However, much uncertainty remains because of the absence of critical evidence of eclogite-facies metamorphism to the east of the Sulu region.

In the Omi eclogite unit, the preliminary phengite ^{40}Ar-^{39}Ar age for pelitic schist accompanying eclogite, and the phengite K-Ar age for fine-grained epidote blueschist give a cooling age of 348–343 Ma (Tsujimori et al., 2001). These are more than 100 m.y. older than phengite ^{40}Ar-^{39}Ar ages from UHP metamorphic rocks in east-central China (230–190 Ma; Eide et al., 1994; Hacker and Wang, 1995). However, the Qinling-Dabie fold belt is composed not only of major Permian–Triassic units, but also a Late Paleozoic ophiolite-bearing accretionary complex (e.g., Maruyama et al., 1994). Recently, Xu et al. (2000) reported phengite ^{40}Ar-^{39}Ar ages of 430–350 Ma from an eclogite-bearing unit in the northwestern part of the Dabie region. It is reasonable to expect continuous subduction of oceanic crust and subsequent exhumation of high-pressure rocks prior to cratonal collision. Therefore, the eclogite-bearing Renge metamorphic belt in southwestern Japan may be a candidate for the eastern extension of the suture zone in east-central China. If so, the Late Paleozoic blueschist and eclogite metamorphism in the Renge metamorphic belt suggests that oceanic crust between the Sino-Korean and Yangtze blocks subducted until collision and underthrusting of the Yangtze block occurred.

Acknowledgments

This research was supported financially in part by the JSPS Research Fellowship for Young Scientists. The author wishes to thank his many colleagues for many helpful suggestions during the course of this study. The author is much indebted to A. Ishiwatari, H. Shukuno, H. Itoh, and C. Gouzu for their help in geochemical analyses and field work. The author is also grateful to S. Banno for providing his locality map of glaucophane schist in the Omi area. The manuscript was improved by critical reviews and comments from B. W. Evans, S. Banno, and J. G. Liou.

REFERENCES

Arakawa, Y, Saito, Y., and Amakawa, H., 2000, Crustal development of the Hida belt, Japan: Evidence from Nd-Sr isotopic and chemical characteristics of igneous and metamorphic rocks: Tectonophysics, v. 328, p. 183–204.

Banno, S., 1958, Glaucophane schists and associated rocks in the Omi district, Niigata Prefecture, Japan: Japanese Journal of Geology and Geography, v. 29, p. 29–44.

Carswell, D. A., O'Brien, P. J., Wilson, R. N. and Zhai, M., 1997, Thermobarometry of phengite-bearing eclogites

in the Dabie Mountains of central China: Journal of Metamorphic Geology, v. 15, p. 239–252.

Eide, E. A., McWilliams, M. O., and Liou, J. G., 1994, $^{40}Ar/^{39}Ar$ geochronology and exhumation of high-pressure to ultrahigh-pressure metamorphic rocks in east-central China: Geology, v. 22, p. 601–604.

Ernst, W. G., 1988, Tectonic history of subduction zones inferred from retrograde blueschist P-T paths: Geology, v. 16, p. 1081–1084.

Ernst, W. G., and Liou, J. G., 1995, Contrasting plate-tectonic styles of the Qinling-Dabie-Sulu and Franciscan metamorphic belts: Geology, v. 23, p. 353–356.

Ernst, W. G., Zhou, G., Liou, J. G., Eide, E., and Wang, X., 1991, High-pressure and superhigh-pressure metamorphic terranes in the Qinling-Dabie Mountain Belt, central China; Early- to Mid-Phanerozoic accretion of the western paleo-Pacific rim: Pacific Science Association Information Bulletin, v. 43, p. 6–14.

Evans, B. W., 1990, Phase relations of epidote-blueschists: Lithos, v. 25, p. 3–23.

Goto, A., Higashino, T., and Sakai, C., 1996, XRF analyses of Sanbagawa pelitic schists in central Shikoku, Japan: Memoirs of the Faculty of Science, Kyoto Univ., Series of Geology and Mineralogy. no. 58, p. 1–19.

Gómez-Pugnaire, M-T., Karsten, L. and Sanchez-Vizcaino, V. L., 1997, Phase relationships and P-T conditions of coexisting eclogite-blueschists and their transformation to greenschist-faciesrocks in the Nerkau Complex (Northern Urals): Tectonophysics, v. 276, p. 195–216.

Guillot, S., de Sigoyer, J., Lardeaux, J. M., and Mascle, G., 1997, Eclogitic metasediments from the Tso Morari area (Ladakh, Himalaya): Evidence for continental subduction during India-Asia convergence: Contributions to Mineralogy and Petrology, v. 128, p. 197–212.

Guiraud, M., Holland, T. and Powell, R., 1990, Calculated mineral equilibria in the greenschist-blueschist-eclogite facies in Na_2O-FeO-MgO-Al_2O_3-SiO_2-H_2O; methods, results, and geological applications: Contributions to Mineralogy and Petrology, v. 104, p. 85–98.

Hacker, B. R., 1996, Eclogite formation and the rheology, buoyancy, seismicity, and H_2O content of oceanic crust, *in* Bebout, G. E. et al., eds., Subduction top to bottom: American Geophysical Union, Geophysical Monograph, no. 96, p. 337–346.

Hacker, B. R., and Wang, Q., 1995, Ar/Ar geochronology of ultrahigh-pressure metamorphism in central China: Tectonics, v. 14, p. 994–1006.

Hirajima, T., Ishiwatari, A., Cong, B., Zhang, R., Banno, S., and Nozaka, T., 1990, Coesite from Mengzhong eclogite at Donghai country, northeastern Jiangsu province, China: Mineralogical Magazine, v. 54, p. 579–583.

Hiroi, Y., 1981, Subdivision of the Hida metamorphic complex, central Japan, and its bearing on the geology of the Far East in pre-Sea of Japan time: Tectonophysics, v. 76, p. 317–333.

_____, 1983, Progressive metamorphism of the Unazuki pelitic schists in the Hida terrane, central Japan: Contributions to Mineralogy and Petrology, v. 82, p. 334–350.

Holland, T. J. B., 1979, The experimental determination of the reaction paragonite = jadeite + kyanite + H_2O and internally consistent thermodynamic data for part of the system Na_2O-Al_2O_3-SiO_2-H_2O, with applications to eclogites and blueschists: Contributions to Mineralogy and Petrology, v. 68, p. 293–301.

_____, 1980, The reaction albite = jadeite + quartz determined experimentally in the range 600–1200°C: American Mineralogist, v. 65, p. 125–134.

Isozaki, Y., 1996, Anatomy and genesis of a subduction-related orogen: A new view of geotectonic subdivision and evolution of the Japanese Island: The Island Arc, v. 5, p. 289–320.

_____, 1997, Contrasting two types of orogen in Permo-Traissic Japan: Accretionary versus collisional: The Island Arc, v. 6, p. 2–24.

Kobayashi, T., 1941, The Sakawa orogenic cycle and its bearing on the origin of the Japanese Islands. Jour. Fac. Sci., Imperial Univ. of Tokyo, Section II, no. 5, p. 219–578.

Komatsu, M., 1990, Hida "Gaien" belt and Joetsu belt, *in* Ichikawa, K., ed., Pre-Cretaceous terranes of Japan: Osaka, Japan, IGCP Project 224, p. 25–40.

Komatsu, M., Nagase, M., Naito, K., Kanno, T., Ujihara, M., and Toyoshima, T., 1993, Structure and tectonics of the Hida massif, central Japan: Memoirs of the Geological Society of Japan, no. 42, p. 39–62. (in Japanese with English abstract)

Krogh, E. J., 1988, The garnet-clinopyroxene Fe-Mg geothermometer—a reinterpretation of existing experimental data: Contributions to Mineralogy and Petrology, v. 75, p. 387–393.

Krogh, E. J., Oh, C. W., and Liou, J. G., 1994, Polyphase and anticlockwise P-T evolution for Franciscan eclogites and blueschists from Jenner, California, USA: Journal of Metamorphic Geology, v. 12, p. 121–134.

Kumazaki, N., and Kojima, S., 1996, Depositional history and structural development of the Kuruma Group (lower Jurassic) on the basis of clastic rock composition: Journal of the Geological Society of Japan, v. 102, p. 285–302 (in Japanese with English abstract).

Kunugiza, K., Sohma, T., Yamamoto, K., Sode, M., Takeda, T., Kawai, A., and Itaya, T., 1997, A structural model of the Hida marginal belt constrained by the petrology and geochronology of metamorphic rocks, *in* Petrologic and geochronologic examination of the metamorphic rocks in the Hida marginal belt: Report of Scientific Project, Grand-in-aid for Scientific Res. (C), p. 25–32 (in Japanese).

Kunugiza, K., Tsujimori, T. and Kano, T., 2001, Developments of the Hida and Hida marginal belts, *in* Kano, T., ed., ISRGA field guidebook for major geologic units of southwest Japan—excursion guidebook for the field

workshop of International Symposium on the Assembly and Breakup of Rodinia and Gondwana, and Growth of Asia, p. 75–131.

Leake, B. E., 1978, Nomenclature of amphibole: American Mineralogist, v. 63, p. 1023–1052.

Lee, S. R., Cho, M., Yi, K., and Stern, R. A., 2000, Early Proterozoic granulites in central Korea: Tectonic correlation with Chinese cratons: Journal of Geology, v. 108, p. 729–738.

Maruyama, S., 1997, Pacific-type orogeny revisited: Miyashiro-type orogeny proposed: The Island Arc, v. 6, p. 91–120.

Maruyama, S., Liou, J. G., and Zhang, R. Y., 1994, Tectonic evolution of the ultrahigh-pressure (UHP) and high-pressure (HP) metamorphic belts from central China: The Island Arc, v. 3, p. 112–121.

Matsumoto, K., 1980, Serpentinite melange of the Omi area, Hida marginal zone, *in* Hida-Gaien Belt: Grant-in-aid for Scientific Res. (A), no. 1, p. 1–14 (in Japanese).

Miyashiro, A., 1957, The chemistry, optics, and genesis of the alkali-amphiboles: Journal of the Faculty of Science, University of Tokyo, Section II, no. 10, p. 57–83.

_____, 1961, Evolution of metamorphic belts: Journal of Petrology, v. 2, p. 277–311.

Morimoto, N., Fabries, J., Ferguson, A. K., Ginzburg, I. V., Ross, M., Seifert, F. A., Zussman, J., Aoki, K., and Gottardi, G., 1988, Nomenclature of pyroxenes: American Mineralogist, v. 73, p. 1123–1133.

Nakamizu, M., Okada, M., Yamazaki, T., and Komatsu, M., 1989, Metamorphic rocks in the Omi-Renge serpentinite melange, Hida Marginal Tectonic Belt, Central Japan: Memoirs of the Geological Society of Japan, no. 33, p. 21–35 (in Japanese with English abstract).

Nishimura, Y., 1998, Geotectonic subdivision and areal extent of the Sangun belt, Inner Zone of Southwest Japan: Journal of Metamorphic Geology, v. 16, p. 129–140.

Patrick, B. E., and Evans, B. W., 1989, Metamorphic evolution of the Seward Peninsula blueschist terrane: Journal of Petrology, v. 30, p. 531–558.

Peacock, S. M., 1993, Metamorphism, dehydration, and the importance of the blueschist eclogite transition in subducting oceanic crust: Geological Society of America Bulletin, v. 105, p. 684–694.

Pearce, J. A., 1982, Trace element characteristics of lavas from destructive plate bounders, *in* Thorpe, R. S., ed., Andesites: orogenic andesites and related rocks: New York, NY: John Wiley and Sons, Inc., p. 525–548.

_____, 1983, The role of sub-continental lithosphere in magma genesis at disructive plate margins, *in* Howkesworth, C. J., and Norry, M. J., eds., Continental basalts and mantle xhenoliths: Nantwich, UK, Shiva Publishing, p. 230–249.

Ree, J.-H., Cho, M., Kwon, S.-T., and Nakamura, E., 1996, Possible eastward extension of Chinese collision belt in South Korea; the Imjingang Belt: Geology, v. 24, p. 1071–1074.

Schliestedt, M., 1986, Eclogite-blueschist relationships as evidenced by mineral equilibria in the high-pressure metabasic rocks of Sifnos (Cycladic Islands), Greece: Journal of Petrology, v. 27, p. 1437–1459.

Shibata, K., and Nozawa, T., 1968, K-Ar age of Omi schist, Hida mountains, Japan: Bulletin of the Geological Survey of Japan, no. 19, p. 243–246.

Sohma, T., and Kunugiza, K., 1993, The formation of the Hida nappe and the tectonics of Mesozoic sediments: The tectonic evolution of the Hida region, Central Japan: Memoirs of the Geological Society of Japan, no. 42, p. 1–20 (in Japanese with English abstract).

Sun, S. S., and McDonough, W. E., 1989, Chemical and isotopic systematics of ocean basalts: Implications for mantle composition and processes, *in* Saunders, A. D., and Norry, M. J., eds., Magmatism in the ocean basins: Geological Society of London Special Publication, no. 42, p. 313–345.

Suzuki, M., Nakazawa, S., and Osakabe, T., 1989, Tectonic development of the Hida belt—with special reference to its metamorphic history and late Carboniferous to Triassic orogenies: Memoirs of the Geological Society of Japan, no. 33, p. 1–10 (in Japanese with English abstract).

Thompson, J. B., 1957, The graphical analysis of mineral assemblages in pelitic schist: American Mineralogist, v. 42, p. 842–858.

Tsujimori, T., 2001, Database on rock-forming minerals (1): Na amphibole from Renghe schist at Osayama, Wakasa, Oya, Hakogase and Omi areas, SW Japan: Bulletin of the Research Institute of Natural Science, Okayama University of Science, no. 27, p. 37–92.

Tsujimori, T., Hyoudo, H., and Itaya, T., 2001, $^{40}Ar/^{39}Ar$ phengite age constrains on the exhumation of the eclogite facies rocks in the Renghe metamorphic belt, SW Japan [abs.]: 2001 Japan Earth and Planetary Science Joint Meeting, Tokyo, Japan (CD-ROM).

Tsujimori, T., Ishiwatari, A. and Banno, S., 2000a, Discovery of eclogitic glaucophane schist from the Omi area, Renge metamorphic belt, the Inner Zone of southwestern Japan: Journal of the Geological Society of Japan, v. 106, p. I–II.

_____, 2000b, Eclogitic glaucophane schist from the Yunotani valley in Omi Town, the Renge metamorphic belt, the Inner Zone of southwestern Japan: Journal of the Geological Society of Japan, v. 106, p. 353–362 (in Japanese with English abstract).

Tsujimori, T., and Itaya, T., 1999, Blueschist-facies metamorphism during Paleozoic orogeny in southwestern Japan: Phengite K-Ar ages of blueschist-facies tectonic blocks in a serpentinite melange beneath Early Paleozoic Oeyama ophiolite: The Island Arc, v. 8, p. 190–205.

Wang, X., Zhang, R., and Liou, J. G., 1995, UHPM terrane in East Central China, *in* Coleman, R. G., and Wang,

X., eds, Ultrahigh pressure metamorphism: Cambridge, UK, Cambridge University Press, p. 356–390.
Xu, B., Grove, M., Wang, C., Zhang, L., and Liu, S., 2000, $^{40}Ar/^{39}Ar$ thermochronology from the northwestern Dabie Shan: Constrains on the evolution of Qinling-Dabie orogenic belt, east-central China: Tectonophysics, v. 322, p. 279–301.
Yokoyama, K., Brothers, R. N., and Black, P. M., 1986, Regional eclogite facies in the high-pressure metamorphic belt of New Caledonia: Geological Society of America, Memoir no. 164, p. 407–423.